BIOMOLECULES & THERAPEUTICS

Original Article
Biomol Ther 30(4), 340-347 (2022)

PRR16/Largen Induces Epithelial-Mesenchymal Transition through the Interaction with ABI2 Leading to the Activation of ABL1 Kinase

Gyeoung Jin Kang[1,†], Jung Ho Park[2,†], Hyun Ji Kim[2], Eun Ji Kim[1], Boram Kim[2], Hyun Jung Byun[2], Lu Yu[2], Tuan Minh Nguyen[2], Thi Ha Nguyen[2], Kyung Sung Kim[2], Hiệu Phùng Huy[2], Mostafizur Rahman[2], Ye Hyeon Kim[2], Ji Yun Jang[2,3], Mi Kyung Park[3], Ho Lee[3], Chang Ick Choi[2], Kyeong Lee[2], Hyo Kyung Han[2], Jungsook Cho[2], Seung Bae Rho[3,*] and Chang Hoon Lee[2,*]

[1]*Lillehei Heart Institute, University of Minnesota, Minneapolis, MN 55455, USA*
[2]*College of Pharmacy, Dongguk University, Goyang 10326,*
[3]*National Cancer Center, Goyang 10408, Republic of Korea*

Abstract

Advanced or metastatic breast cancer affects multiple organs and is a leading cause of cancer-related death. Cancer metastasis is associated with epithelial-mesenchymal metastasis (EMT). However, the specific signals that induce and regulate EMT in carcinoma cells remain unclear. PRR16/Largen is a cell size regulator that is independent of mTOR and Hippo signalling pathways. However, little is known about the role PRR16 plays in the EMT process. We found that the expression of PRR16 was increased in mesenchymal breast cancer cell lines. PRR16 overexpression induced EMT in MCF7 breast cancer cells and enhances migration and invasion. To determine how PRR16 induces EMT, the binding proteins for PRR16 were screened, revealing that PRR16 binds to Abl interactor 2 (ABI2). We then investigated whether ABI2 is involved in EMT. Gene silencing of ABI2 induces EMT, leading to enhanced migration and invasion. ABI2 is a gene that codes for a protein that interacts with ABL proto-oncogene 1 (ABL1) kinase. Therefore, we investigated whether the change in ABI2 expression affected the activation of ABL1 kinase. The knockdown of ABI2 and PRR16 overexpression increased the phosphorylation of Y412 in ABL1 kinase. Our results suggest that PRR16 may be involved in EMT by binding to ABI2 and interfering with its inhibition of ABL1 kinase. This indicates that ABL1 kinase inhibitors may be potential therapeutic agents for the treatment of PRR16-related breast cancer.

Key Words: PRR16, ABI2, ABL1 kinase, Epithelial-mesenchymal transition, Breast cancer

INTRODUCTION

Advanced or metastatic breast cancer affects multiple organs and is a leading cause of cancer death (Jones, 2008; Peart, 2017). For example, despite advances in breast cancer screening, diagnosis, and treatment, nearly 12% of patients diagnosed with breast cancer eventually develop metastatic disease or breast cancer that spreads beyond the breast to other parts of the body (Peart, 2017). Treatments for metastatic breast cancer are still lacking, thus it generally has a poor prognosis, with a 5-year survival rate of 26% (Peart, 2017). Common sites of metastasis include the bone, liver, lung, brain, lymph nodes, pleura, and skin (Lu and Kang, 2007; Kennecke *et al*., 2010). Interestingly, breast cancer-specific subtypes (i.e., luminal A and B, HER2 enriched and basal-like) have preferential metastasis sites, with both the tumour cells and metastatic microenvironment possibly contributing to this organ specificity (Lu and Kang, 2007; Guo and Deng, 2018). However, to date, the biology of breast cancer metastasis according to the organ site remains largely unknown.

Epithelial−mesenchymal metastasis (EMT) is a cellular process that is known to play a key role in metastasis. In this process, epithelial cells experience the loss of cell-cell and cell-stromal junctions, adopt a mesenchymal cell shape, and

Open Access **https://doi.org/10.4062/biomolther.2022.066**

Received May 15, 2022 **Revised** May 28, 2022 **Accepted** Jun 1, 2022
Published Online Jun 20, 2022

***Corresponding Authors**
E-mail: sbrho@ncc.re.kr (Rho SB), uatheone@dongguk.edu (Lee CH)
Tel: +82-31-920-2383 (Rho SB), +82-31-961-5213 (Lee CH)
Fax: +82-31-920-2399 (Rho, SB), +82-31-961-5206 (Lee CH)
[†]The first two authors contributed equally to this work.

exhibit dedifferentiation, migration, and invasive behaviour (Brabletz *et al*., 2018; Lee, 2018). In the past few decades, activation of the EMT program has been proposed as an important mechanism for the development of a malignant phenotype in epithelial cancer cells. However, the specific signals that induce and regulate EMT in carcinoma cells require further analysis (Lee, 2019).

PRR16/Largen is a cell size regulator that is independent of mTOR and Hippo signalling pathways (Yamamoto *et al*., 2014). It works by stimulating the translation of certain mRNAs, including those encoding proteins that affect mitochondrial function, leading to an increase mitochondrial mass and respiration. It has been reported that the expression of PRR16 is higher in liver cancer tissues and carotid paragangliomas (Snezhkina *et al*., 2019; Bai *et al*., 2020). However, its role in the EMT process remains unclear.

In this report, we find that PRR16 may be involved in the EMT process of breast cancer via the PRR16/Abl interactor 2 (ABI2)/ABL1 axis. This indicates that ABL1 kinase inhibitors could be employed as therapeutic agents for the treatment of PRR16-related breast cancer.

MATERIALS AND METHODS

Materials

High-glucose Dulbecco's Modified Eagle Medium (DMEM), fetal bovine serum (FBS), phosphate-buffered saline (PBS), and antibiotics (penicillin and streptomycin; P/S) were purchased from Welgene Inc. (Gyeongsan, Korea). Antibody against PRR16 (PA5-61919) was purchased from LSBio (Seattle, WA, USA). Antibodies against vimentin (sc-32322), and β-actin (sc-47778) were purchased from Santa Cruz Biotechnology (Santa Cruz, CA, USA). Antibodies against N-cadherin (ab12221), and Snail (ab167609) were purchased from Abcam (Cambridge, UK). Anti-E-cadherin (610181), phycoerythrin (PE)-conjugated CD24 (555482), and allophycocyanin (APC)-conjugated CD44 antibodies were purchased from BD Biosciences (Palo Alto, CA, USA). Anti-mouse-horseradish peroxidase (HRP) and anti-rabbit-fluorescein isothiocyanate (FITC)-labeled 2nd antibodies were obtained from Santa Cruz Biotechnology. Anti-rabbit-HRP and anti-mouse-Alexa594 conjugated antibodies were bought from GenDEPOT, Inc. (Barker, TX, USA) and Thermo Fisher Scientific (Rockford, IL, USA), respectively. All of the other chemicals were of reagent grade.

Cell culture and stable cell lines generation

All cell lines were obtained from the American Type Culture Collection (Bethesda, MD, USA). Human breast cancer cell lines, MCF7 and MDA-MB-231, were cultured in high glucose DMEM with 10% FBS and 1% P/S in a humidified CO2 incubator (Kang *et al*., 2017). Human mammary epithelial cell line, MCF10A, was maintained in DMEM/F-12 medium supplemented with 5% horse serum, 0.5 μg/mL hydrocortisone, 10 μg/mL insulin, 20 ng/mL epidermal growth factor, 1% P/S. To generate PRR16 knockdown or overexpressing cell lines, lentiviruses encoding control or PRR16 short hairpin RNA and empty or PRR16 pcDNA3.1 vector were transduced into target cells. Then, the cells were selected and maintained by puromycin or G418 selection protocol.

siRNA or plasmid DNA transfection

For gene-knockdown assay, cells were transfected with control or PRR16 siRNA (sequence: 5'-GCUGCAUACCCAACAGUAA-3', ST Pharm, Seoul, Korea) using Lipofectamine™ 2000 Transfection Reagent (Invitrogen, Waltham, MA, USA), following the manufacturer's protocol. The ratio of siRNA vs lipofectamine reagent was 1:1.5. For transient over-expression assay, PRR16 cDNA was cloned into pcDNA3.1 vector. 70-80% confluent cells were transfected using JetPEI (Polyplus Transfection, San Marcos, CA, USA), according to the manufacturer's recommendations (DNA:JetPEI=1:2). After 24 h of transfection, the cells were used in further experiments.

RNA preparation and polymerase chain reaction (PCR)

Total RNA was prepared using TRIzol® RNA Isolation Reagents (Invitrogen) according to the manufacturer's instructions (Rho *et al*., 2021b). Reverse transcription was performed with a First Strand cDNA Synthesis kit (Promega, Madison, WI, USA). The reverse transcription PCR reaction was performed in the 96-Well GeneAmp® PCR System 9700 (Applied Biosystems, Piscataway, NJ, USA) using AccuPower® HotStart PCR PreMix (Bioneer, Daejeon, Korea) with the appropriate sense and antisense primers. The primer sequence was as follows: N-cadherin (F: 5'-ATCCGGT- CCGATCTGCAGCC-3'; R: 5'-GTGGCCCCCAGTCGTT- CAGGTA-3'; 198 bp), Vimentin (F: 5'-ACCAAGACA CTATTGGCCGCCT-3'; R: 5'-CCCTCAGGTTCAGGGAGGAAAAGT-3'; 201 bp), E-cadherin (F: 5'-TGCCCAGAAAATGAAAAAGG-3'; R: 5'-GTGTATGT- GG CAATGCGTTC-3'; 200 bp), PRR16 (F: 5'-CAGTGGTGCTGCCATCAACT -3'; R: 5'- TTTGCTTTTGTCATTAT-3'; 200 bp), Snail (F: 5'-AGCCTGGGTGCCC- TCAAGATG-3'; R: 5'-CTTGGTGCTTGTGGAGCAGGGAC-3'; 274 bp), and β-actin (F: 5'-TGAAGCTGAGGG- AGCCACAGC-3'; R: 5'-GGGTTCTCCCT- GGGCACCAA-3'; 540 bp). The reaction products were visualized by electrophoresis on a 1.2% agarose gel (Invitrogen) under UV light illumination after staining with SafePinky DNA Gel Staining Solution (GenDEPOT, Inc.).

Western blot analysis

Cells were washed twice with ice-cold PBS and disrupted in RIPA buffer with Xpert Protease Inhibitor Cocktail Solution and Xpert Phosphatase Inhibitor Cocktail Solution (GenDEPOT, Inc.) on ice for 30 min (Rho *et al*., 2021a). Cell lysates were centrifuged at 15,000 rpm for 15 min at 4°C, and the resultant supernatants were subjected to Western blotting. The total protein concentration was quantified using the Pierce BCA Protein Assay Kit (Thermo Fisher Scientific). Proteins were separated by electrophoresis on a (8-10)% (SDS-PAGE, after which samples were transferred onto a polyvinylidene difluoride (PVDF) membrane. The membrane was treated with 5% skim milk for 1 h and incubated overnight at 4°C with the appropriate primary antibodies. After TBST washing, the membrane was incubated with HRP-conjugated secondary antibody (1:5,000) for 90 min at RT. The bands were visualized using PowerOpti-ECL detection reagent (Animal Genetics Inc., Suwon, Korea).

Co-immunoprecipitation

A total of 1 mg of cell lysate was incubated for 1 h with IgG and 10 μg of protein A/G beads. The lysate was incubated overnight at 4°C with 2 μg of anti-PRR16 antibodies or anti-ABI2 antibodies or nonspecific IgGs. Then, lysate was incu-

bated once more for 2 h at 4°C with 20 μg protein A/G agarose beads (50% slurry; Thermo Fisher Scientific). The samples were then centrifuged, and the pellets were washed with 1 mL of the lysate buffer (10 mM Tris-HCl, pH7.4, 150 mM NaCl, 5 mM EDTA, 0.1% Triton X-100). The immunoprecipitated proteins were extracted by 10 min boiling with 2 × Laemmli 40 μL and detected by immunoblot with anti-PRR16 or anti-ABI2 antibodies.

Confocal microscopy analysis

Cells were seeded on coverslips, and incubated with EMT conditions. The cells were washed with ice-cold PBS and fixed in 4% paraformaldehyde for 10 min at RT. The cells were then permeabilized with 0.1% Triton X-100 for 10 min, blocked with 3% BSA for 30 min, and incubated with primary antibodies overnight at 4oC. After PBS washing, the cells were incubated with fluorescence conjugated secondary antibodies for 1 h at RT. Finally, the samples were mounted onto slide with DAPI contained solution and visualized using a Nikon's C1 plus Digital Eclipse Modular Confocal Microscope System (Nikon Instruments Inc., Tokyo, Japan).

Migration and invasion assay

Cell migration assay were performed using ChemoTx micro plate 96-well (Neuro Probe, Inc., Gaithersburg, MD, USA) (Nam *et al*., 2022). The bottom side of the ChemoTx membrane was pre-coated with fibronectin (10 μg/mL). Then the lower chamber was filled by 10% serum media and the cells in serum-free media were placed directly into the upper side of membrane. After incubation, the migrated cells were stained with Diff Quick® Stain reagents (Sysmex, Kobe, Japan). For the transwell invasion assay, the upper chamber was pre-coated with Matrigel (1 mg/mL). Then the cells in 0.2 mL medium without serum were placed in the upper chamber, and the lower chamber was filled with 0.6 mL of medium with 10% serum. Following an incubation period, the cells opposite the upper chamber were fixed, and stained with hematoxylin and eosin stain solution. Cells in four different fields of view were counted.

Statistical analysis

Student's t-test was used to determine the statistical significance of the differences between the experimental and control group values. The data presented represent the mean ± standard deviation.

RESULTS

Expression of PRR16 in Breast Cancer Cells

Initially we explored whether PRR16 expression was involved in the progression of breast cancer. To investigate the prognostic significance of PRR16 mRNA expression in breast cancer, survival analysis was conducted using an online Kaplan Meier-plotter. Breast cancer patients were divided into two subgroups, PRR16-high and PRR16-low, on the basis of their quartile expression levels. There was a significant difference in the probability of overall survival in the patients group with a positive lymph node status (*p* value=0.0, HR (95% CI)=2.21 (1.57-3.11), n=1067) (Fig. 1A, left) and in the patients group with a basal subtype and no systematic treatment (*p* value=0.00, HR (95% CI)=5.28 (2.49-11.22), n=71) (Fig. 1A, right).

The expression of PRR16 in breast cancer cell lines was positively correlated with the expression of PRR16 and inversely correlated with the expression of CDH1 (Fig. 1B). The expression of PRR16 in the microarray data sets (GSE10890) was also found to be higher in the basal-type breast cancer cell line (Fig. 1C). The expression of PRR16 in the epithelial and mesenchymal breast cancer cell lines was investigated using the GSE66527 microarray data set. PRR16 was higher in the mesenchymal cell lines with the expression of mesenchymal markers including vimentin, ZEB1 and ZEB2. In contrats, the expression of PRR16 was lower in the epithelial cell lines (Fig. 1D).

To gain further insight from the microarray data, we conducted gene set enrich analysis (GSEA) using the whole microarray gene list (high PRR16 expression vs low PRR16 expression in basal-type of breast cancer tissues; GSE21653). GSEA can be employed to determine whether an a priori defined set of genes exhibits a statistically significant difference between high and low PRR16 expression. The results showed that the 'HALLMARK_EPITHELIAL_MESENCHYMAL_TRANSITION' gene set was positively enriched in high PRR16 expression tissue (Fig. 1E).

PRR16 induces the epithelial-mesenchymal transition in breast cancer cells

The overexpression of PRR16 in MCF7 and SK-BR-3 cells led to a decrease in cell adhesion in MCF7 cells (Fig. 2A), while the gene silencing of PRR16 in MDA-MB-231 cells increased cell adhesion (Fig. 2A). Changes in EMT markers were observed in PRR16- overexpressed MCF7 and SK-BR-3 cells with a decrease in E-cadherin expression and an increase in both N-cadherin and vimentin expression (Fig. 2B). Conversely, the higher expression of E-cadherin and lower expression of N-cadherin and vimentin were observed in the PRR16 siRNA treated MDA-MB-231 cells (Fig. 2B). In addition, the expression of ZEB1, ZEB2, SNAIL, and SLUG, which are transcription factors for EMT, increased with the overexpression of PRR16 and decreased in MDA-MB-231 cells after the silencing of PRR16 (Fig. 2C). Changes in these EMT markers were also confirmed using confocal microscopy (Fig. 2D). The overexpression of PRR16 increased migration and invasion in the MCF7 and SK-BR-3 cells, while lower PRR16 expression reduced migration and invasion in MDA-MB-231 cells (Fig. 2E).

PRR16 regulates the expression of ABI2 via binding

In order to elucidate the mechanism underlying the effect of PRR16 on EMT, ABI2, while is the binding partner of PRR16, was selected for further analysis from the bioinformatics site (Rolland *et al*., 2014). It was confirmed by coimmunoprecipitation that ABI2 binds to PRR16 (Fig. 3A). Interestingly, the overexpression of PRR16 inhibited the expression of ABI2 (Fig. 3B), a relationship that was also observed via confocal microscopy (Fig. 3B). The decrease in ABI2 expression due to PRR16 overexpression in MCF7 cells was also confirmed using confocal microscopy (Fig. 3C). It was observed that the expression of ABI2 was higher when PRR16 was knocked down in MDA-MB-231 cells (Fig. 3C).

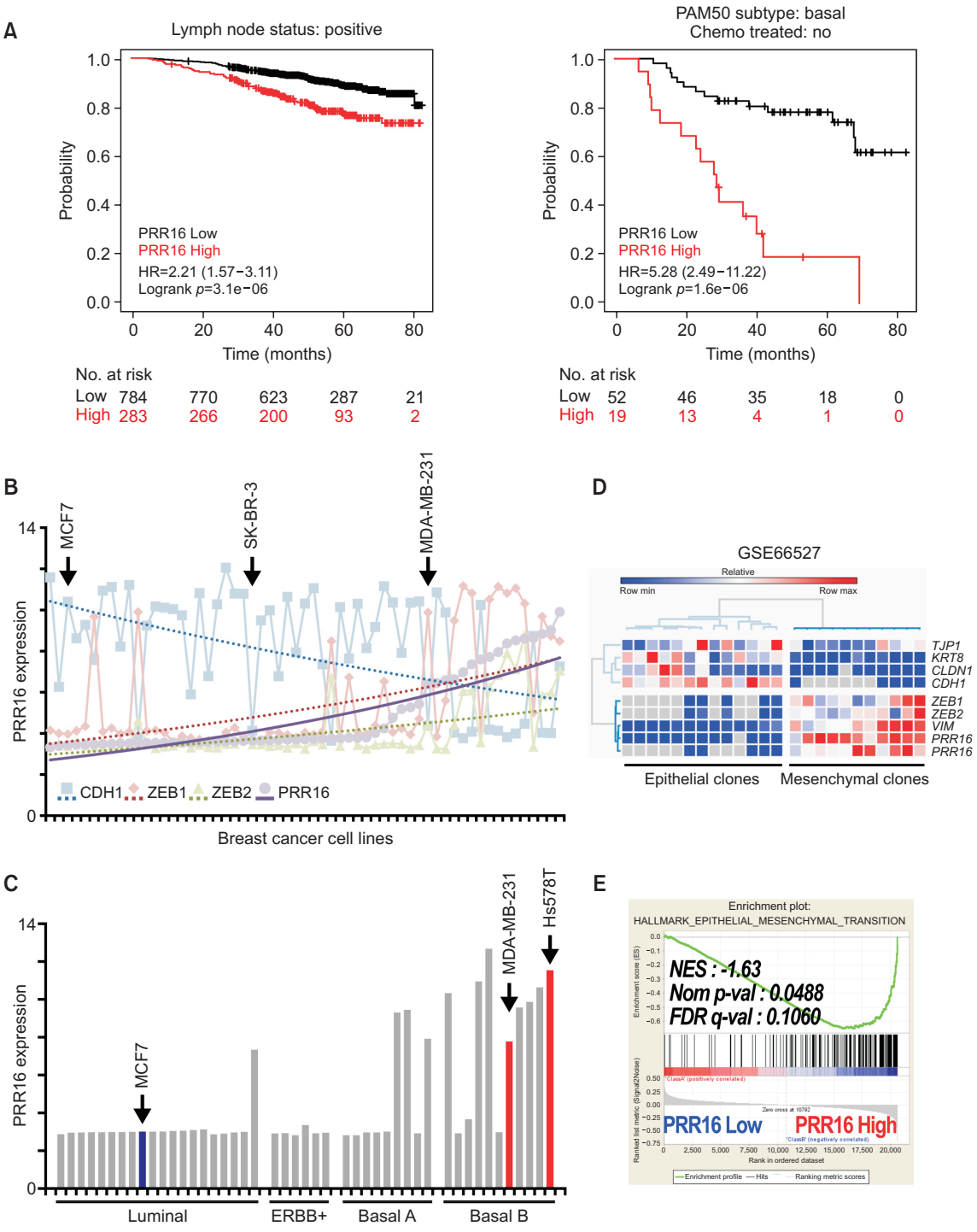

Fig. 1. PRR16 is linked to mesenchymal characteristics. (A) Overall Survival KM plot based on PRR16 expression levels in mRNA RNA-Seq analysis datasets. KM plot based on the PRR16 expression level was expressed in positive lymph node and the basal subtype with no chemo treatment, respectively. (B, C) Expression of PRR16 in breast cancer cell lines examined using Cancer Cell Line Encyclopedia (B) and breast cancer cell line data sets (GSE10890; PRR16 (220014_at)) (C). (D, E) Differential expression pattern for PRR16 in epithelial and mesenchymal breast cancer cell phenotypes. PRR16 expression levels were examined using GSE66527 (D, heatmap) and GSE21653 (E, GSEA).

Loss of ABI2 induces EMT and promotes the phosphorylation of tyrosine 412 of ABL1 kinase

Because PRR16 induces EMT, we investigated whether its binding protein ABI2 was involved in EMT. The si-RNA of ABI2 led to a decrease in E-cadherin expression and an increase in N-cadherin and vimentin expression (Fig. 4A). In addition, lower expression of ABI2 increased the migration and invasion of MCF7 and SK-BR-3 breast cancer cells (Fig.

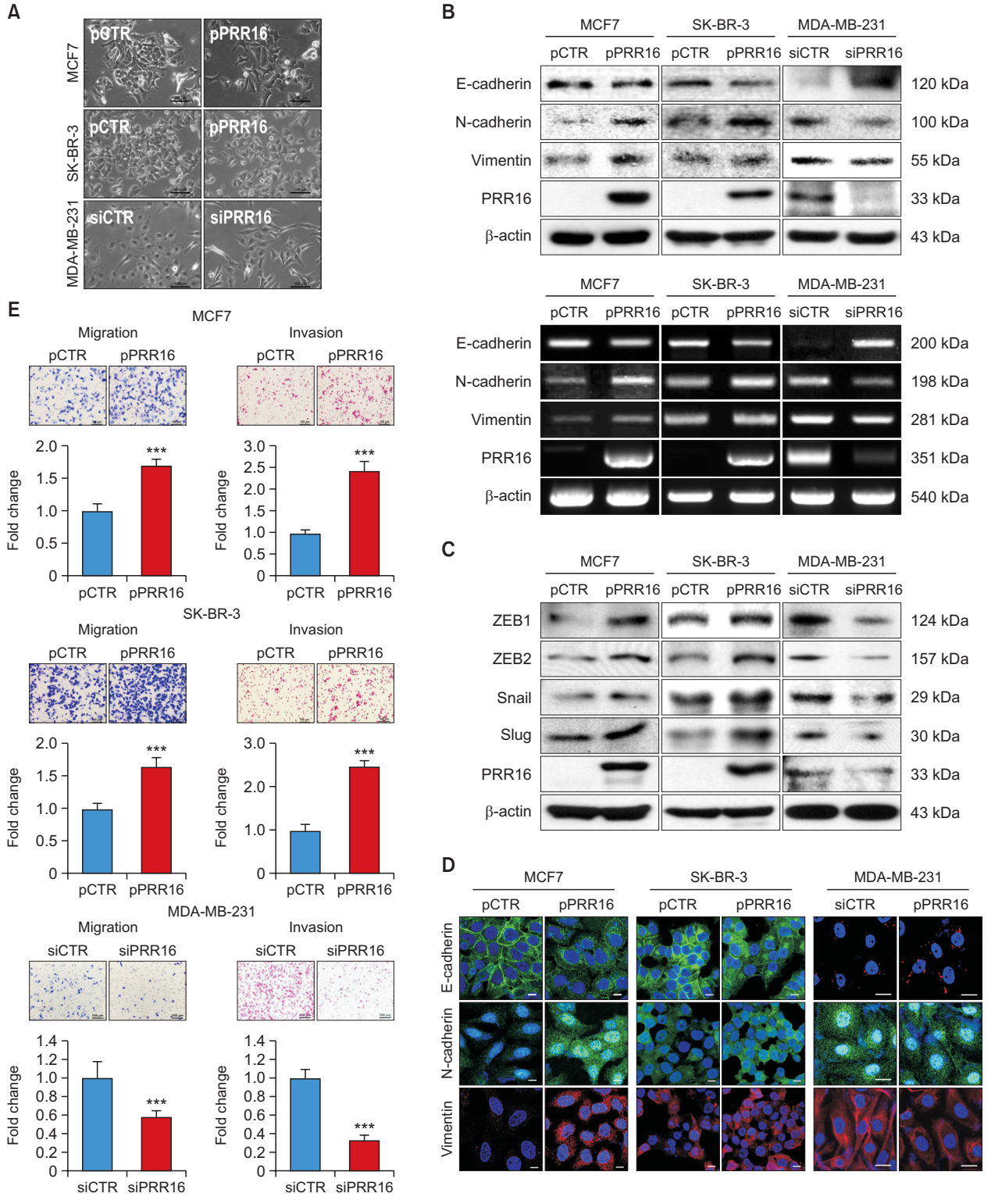

Fig. 2. PRR16 promotes epithelial mesenchymal metastasis in breast cancer cells. (A) Changes in the cell shape in response to PRR16 expression. (B) Effect of PRR16 expression on EMT markers. (C) Effect of PRR16 expression on EMT regulating transcription factors. (D) Confocal image demonstrating the influence of PRR16 expression on EMT markers. (E) Effect of PRR16 expression on cell motility and invasiveness. MCF7 and SK-BR-3 cells were transfected with plasmid DNA to overexpress PRR16, while MDA-MB-231 cells were transfected with siRNA to decrease PRR16 expression. The protein level of the EMT markers and transcription factors were validated by Western blot, and the mRNA levels of the EMT marker were confirmed using PCR. Confocal microscopic analysis validated the protein levels of the EMT markers. Cell migration and invasiveness were assessed using the fibronectin-coated transwell assay and Matrigel-coated transwell assays, respectively. Data are reported as the mean ± SD of three to four independent experiments. ***p<0.001 when compared between the indicated groups using a Student's t-test.

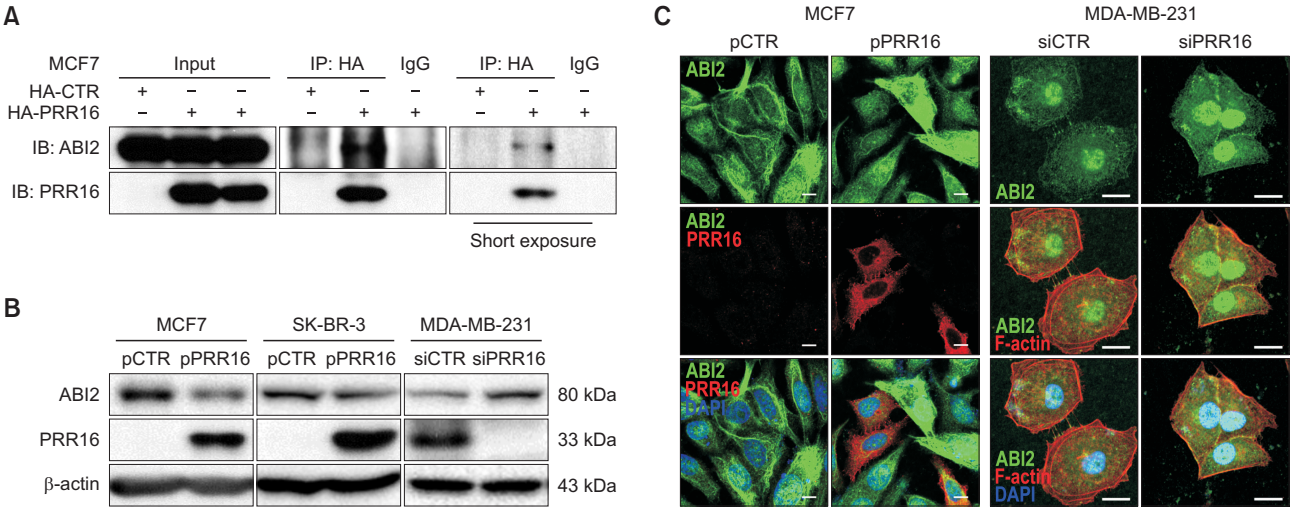

Fig. 3. PRR16 binds to and inhibits ABI2. (A) Confirmation of the interaction between PRR16 and ABI2. (B, C) Effect of PRR16 expression on ABI2 expression. In MCF7 cells, an HA-tagged control (CTR) or PRR16 was overexpressed, and the interaction between PRR16 and ABI2 was verified by immunoprecipitation with HA-specific antibody. MCF7 and SK-BR-3 cells were transfected with plasmid DNA to overexpress PRR16, while MDA-MB-231 cells were transfected with siRNA to decrease PRR16 expression. The protein levels of ABI2, PRR16, β-actin were validated using Western blot. Confocal microscopic analysis validated the protein levels of ABI2.

4B). ABI2 codes for a protein that interacts with ABL1 kinase. Therefore, we investigated whether the change in ABI2 expression affects the activation of ABL1 kinase. As a result of the knockdown of ABI2, it was observed that the phosphorylation of Y412 of ABL1 increased (Fig. 4C). Based on these results, we concluded that PRR16, which interacts with ABI2 and suppresses its expression, also regulates the activity of ABL1 kinase. The effect of ABI2 on the phosphorylation of Y412 in ABL1 was investigated using Western blot analysis. An increase in the expression of PRR16 increased the phosphorylation of Y412 in ABL2 (Fig. 4D). Conversely, reducing the expression of PRR16 led to a reduction in the phosphorylation of ABL1 kinase (Fig. 4D).

DISCUSSION

PRR16 is a gene that has rarely been studied in relation to cancer. However, it is one of the 21 genes with altered expression levels involved in the development of carotid paragangliomas and related to the characteristics of liver cancer stem cell (Snezhkina *et al*., 2019; Bai *et al*., 2020). We found that the expression of PRR16 was high in mesnechymal cell lines, and the fluctuations were high with EMT-related genes in tissues with high PRR16 expression levels (Fig. 1E). These results suggest that PRR16 may be important in EMT. As expected, PRR16 promoted EMT in breast cancer cell lines (Fig. 2). Therefore, in breast cancer patients with high expression of PRR16, PPR16 promotes EMT and thus metastasis, possibly worsening their prognosis, and KMPLOT data supports this (Fig. 1A-1D).

To elucidate the mechanism involved in the promotion of EMT by PRR16, ABI2 was chosen by exploring the interaction partners of PRR16 in the Biogrid (Luck *et al*., 2020). It was confirmed that ABI2 really interacts with PRR16 (Fig. 3). ABI2 has been reported to be a tumour suppressor gene because it is involved in the positive regulation of cell component organization and the regulation of zonula adherens assembly and acts as an inhibitor by binding to ABL kinase (Dai and Pendergast, 1995). Our results show that PRR16 provoked a decrease in the expression of ABI2 through its interaction with ABI2. Therefore, it can be inferred that a decrease in ABI2 expression due to PRR16 leads to the activation of ABL1 kinase, and our results confirmed this (Fig. 4C, 4D). This PRR16-mediated decrease in the expression of ABI2 subsequently led to EMT (Fig. 4A). This is consistent with report of EMT being induced in nasopharyngeal carcinoma cells through the upregulation of c-JUN/SLUG signal following the downregulation of ABI2 expression by EBV-miR-BART13-3p (Huang *et al*., 2020).

The lower expression of ABI2 resulted in the activation of ABL1 kinase, which appears to be involved in inducing EMT. The involvement of ABL1 kinase in EMT has been previously reported in many previous studies. For example, it has been reported that ABLI kinase is involved in epithelial morphology and cadherin swiching in breast cancer cells (Bryce *et al*., 2013). In addition, active ABL kinases promote changes in actin dynamics and promote the remodeling of the adhesion junctions required for EMT (Zandy *et al*., 2007; Zandy and Pendergast, 2008). In addition, ABL kinase activates and promotes the nuclear accumulation of TAZ transcriptional coactivators, which have been shown to promote EMT in breast and lung cancer cells (Lei *et al*., 2008; Gu *et al*., 2016; Wang *et al*., 2016). ABL kinase has also been shown to regulate the expression of the EMT transcription factors ZEB1, TWIST1, SNAIL1, and/or SLUG depending on the cellular context (Allington *et al*., 2009; Suh *et al*., 2013; Jain *et al*., 2017).

The phosphorylation of ABL1-dependent OTULIN (OTU deubiquitinase with linear linkage specificity) induces β-catenin activation following damage to the DNA, promoting drug resistance in triple-negative breast cancer (Wang *et al*., 2020). WNT activation by ABL1 kinase can thus be the main mechanism of action for EMT (Xu *et al*., 2020).

The elusive question that remains is how PRR16 can regu-

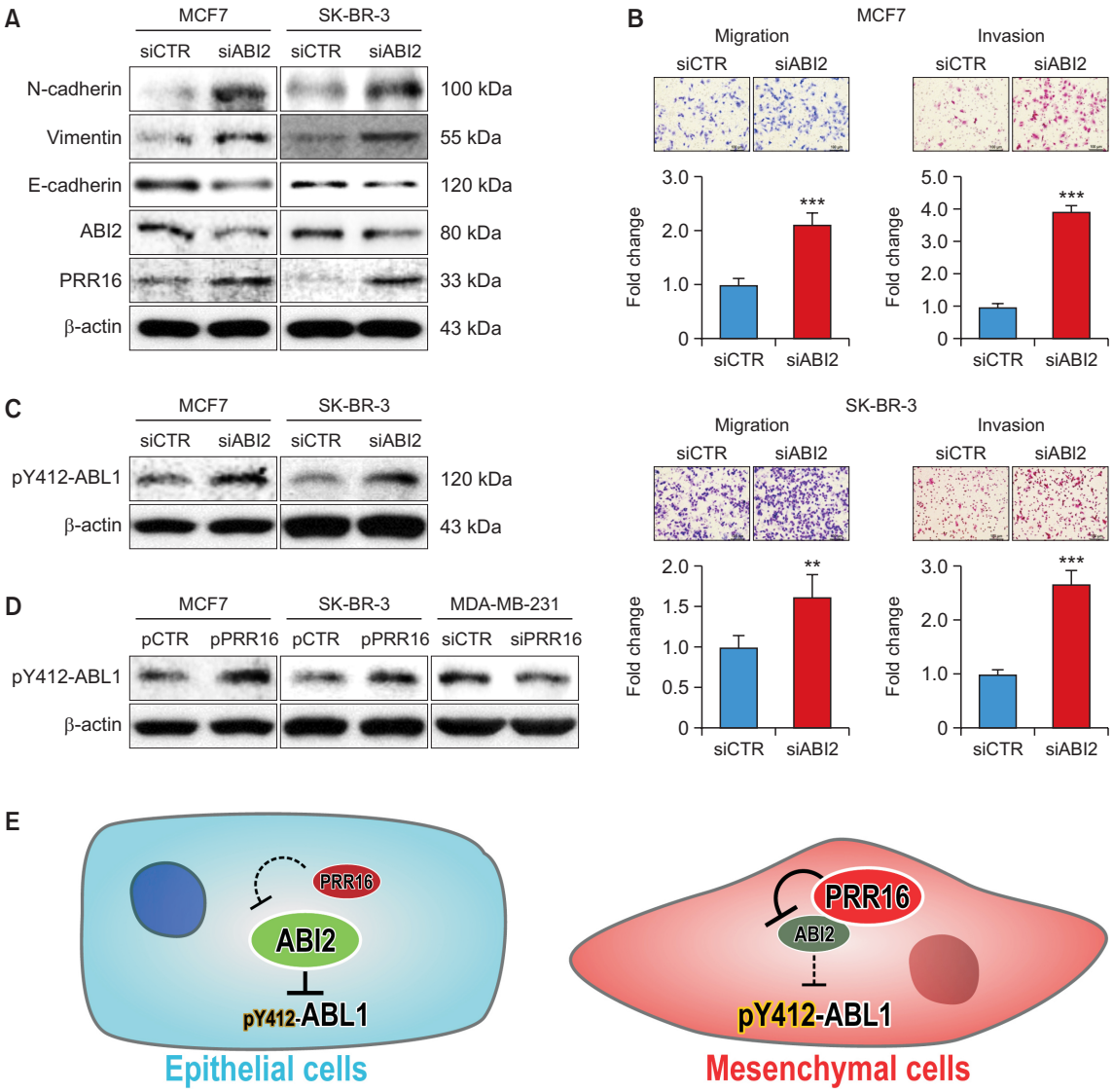

Fig. 4. ABI2 deficiency causes EMT and increases phosphorylation of ABL1 kinase tyrosine 412. (A) Effect of ABI2 expression on EMT markers. (B) Effect of ABI2 expression on cell motility and invasiveness. (C) Effect of ABI2 expression on ABL1 phosphorylation. (D) Effect of PRR16 expression on ABL1 phosphorylation. (E) Mechanism of action of PRR16 via interaction with ABI2 in EMT. MCF7 and SK-BR-3 cells were transfected with siRNA to inhibit ABI2. MCF7 and SK-BR-3 cells were transfected with plasmid DNA to overexpress PRR16, while MDA-MB-231 cells were transfected with siRNA to decrease PRR16 expression. The protein level were validated using Western blot. Cell migration and invasiveness were assessed using fibronectin-coated transwell assay and the Matrigel-coated transwell assay, respectively. Data are presented as the mean ± SD of three to four independent experiments. **p<0.01; ***p<0.001 in comparisons between the indicated groups using a Student's t-test.

late the activity of ABL1 kinase by inducing a decrease in the expression of ABI2. It could be that PRR16 simply competes with ABL1 and binds to ABI2, thus interfering with the ABL1 inhibitory activity of ABI2 or more actively binding with ABI2, leading to degradation (Fig. 4E). It is worth noting that it has been reported in Biogrid that PRR16 binds to E3 ligases such as NEDD4 and NEDD4L (Persaud *et al*., 2009). Research is currently underway to address this question.

In conclusion, in this report, we revealed for the first time that PRR16 can induce EMT via the activation of ABL1 kinase by binding to ABI2. These results are thought to be helpful in suggesting new targets and therapeutic strategies for the control of ABL1-involved cancers.

ACKNOWLEDGMENTS

This study was supported by a grant from the Basic Science Research Program and the BK21 FOUR program through the NRF (NRF-2018R1A5A2023127, NRF-2020R1A2C3004973, NRF-2020R1I1A1A01074006, and NRF-2020M3E5E2038356), the Korea Health Technology R&D Project through the Korea Health Industry Development Institute (KHIDI), funded by the Ministry of Health & Welfare,

Korea (HP20C0131), and the BK21 FOUR program through the National Research Foundation (NRF) of Korea funded by the Ministry of Education (MOE, Korea).

REFERENCES

Allington, T. M., Galliher-Beckley, A. J. and Schiemann, W. P. (2009) Activated Abl kinase inhibits oncogenic transforming growth factor-β signaling and tumorigenesis in mammary tumors. *FASEB J.* **23**, 4231-4243.

Bai, K. H., He, S. Y., Shu, L. L., Wang, W. D., Lin, S. Y., Zhang, Q. Y., Li, L., Cheng, L. and Dai, Y. J. (2020) Identification of cancer stem cell characteristics in liver hepatocellular carcinoma by WGCNA analysis of transcriptome stemness index. *Cancer Med.* **9**, 4290-4298.

Brabletz, T., Kalluri, R., Nieto, M. A. and Weinberg, R. A. (2018) EMT in cancer. *Nat. Rev. Cancer* **18**, 128-134.

Bryce, N. S., Reynolds, A. B., Koleske, A. J. and Weaver, A. M. (2013) WAVE2 regulates epithelial morphology and cadherin isoform switching through regulation of Twist and Abl. *PLoS ONE* **8**, e64533.

Dai, Z. and Pendergast, A. M. (1995) Abi-2, a novel SH3-containing protein interacts with the c-Abl tyrosine kinase and modulates c-Abl transforming activity. *Genes Dev.* **9**, 2569-2582.

Gu, J. J., Rouse, C., Xu, X., Wang, J., Onaitis, M. W. and Pendergast, A. M. (2016) Inactivation of ABL kinases suppresses non–small cell lung cancer metastasis. *JCI insight* **1**, e89647.

Guo, S. and Deng, C. X. (2018) Effect of stromal cells in tumor microenvironment on metastasis initiation. *Int. J. Biol. Sci.* **14**, 2083-2093.

Huang, J., Qin, Y., Yang, C., Wan, C., Dai, X., Sun, Y., Meng, J., Lu, Y., Li, Y. and Zhang, Z. (2020) Downregulation of ABI2 expression by EBV-miR-BART13-3p induces epithelial-mesenchymal transition of nasopharyngeal carcinoma cells through upregulation of c-JUN/SLUG signaling. *Aging (Albany N.Y.)* **12**, 340-358.

Jain, A., Tripathi, R., Turpin, C. P., Wang, C. and Plattner, R. (2017) Abl kinase regulation by BRAF/ERK and cooperation with Akt in melanoma. *Oncogene* **36**, 4585-4596.

Jones, S. E. (2008) Metastatic breast cancer: the treatment challenge. *Clin. Breast Cancer* **8**, 224-233.

Kang, J. H., Kim, H. J., Park, M. K. and Lee, C. H. (2017) Sphingosylphosphorylcholine induces thrombospondin-1 secretion in MCF10A cells via ERK2. *Biomol. Ther. (Seoul)* **25**, 625-633.

Kennecke, H., Yerushalmi, R., Woods, R., Cheang, M. C. U., Voduc, D., Speers, C. H., Nielsen, T. O. and Gelmon, K. (2010) Metastatic behavior of breast cancer subtypes. *J. Clin. Oncol.* **28**, 3271-3277.

Lee, C. H. (2018) Epithelial-mesenchymal transition: initiation by cues from chronic inflammatory tumor microenvironment and termination by anti-inflammatory compounds and specialized pro-resolving lipids. *Biochem. Pharmacol.* **158**, 261-273.

Lee, C. H. (2019) Reversal of epithelial–mesenchymal transition by natural anti-inflammatory and pro-resolving lipids. *Cancers* **11**, 1841.

Lei, Q. Y., Zhang, H., Zhao, B., Zha, Z. Y., Bai, F., Pei, X. H., Zhao, S., Xiong, Y. and Guan, K. L. (2008) TAZ promotes cell proliferation and epithelial-mesenchymal transition and is inhibited by the hippo pathway. *Mol. Cell. Biol.* **28**, 2426-2436.

Lu, X. and Kang, Y. (2007) Organotropism of breast cancer metastasis. *J. Mammary Gland Biol. Neoplasia* **12**, 153-162.

Luck, K., Kim, D. K., Lambourne, L., Spirohn, K., Begg, B. E., Bian, W., Brignall, R., Cafarelli, T., Campos-Laborie, F. J., Charloteaux, B., Choi, D., Coté, A. G., Daley, M., Deimling, S., Desbuleux, A., Dricot, A., Gebbia, M., Hardy, M. F., Kishore, N., Knapp, J. J., Kovács, I. A., Lemmens, I., Mee, M. W., Mellor, J. C., Pollis, C., Pons, C., Richardson, A. D., Schlabach, S., Teeking, B., Yadav, A., Babor, M., Balcha, D., Basha, O., Bowman-Colin, C., Chin, S. F., Choi, S. G., Colabella, C., Coppin, G., D'Amata, C., De Ridder, D., De Rouck, S., Duran-Frigola, M., Ennajdaoui, H., Goebels, F., Goehring, L., Gopal, A., Haddad, G., Hatchi, E., Helmy, M., Jacob, Y., Kassa, Y., Landini, S., Li, R., van Lieshout, N., MacWilliams, A., Markey, D., Paulson, J. N., Rangarajan, S., Rasla, J., Rayhan, A., Rolland, T., San-Miguel, A., Shen, Y., Sheykhkarimli, D., Sheynkman, G. M., Simonovsky, E., Taşan, M., Tejeda, A., Tropepe, V., Twizere, J. C., Wang, Y., Weatheritt, R. J., Weile, J., Xia, Y., Yang, X., Yeger-Lotem, E., Zhong, Q., Aloy, P., Bader, G. D., De Las Rivas, J., Gaudet, S., Hao, T., Rak, J., Tavernier, J., Hill, D. E., Vidal, M., Roth, F. P. and Calderwood, M. A. (2020) A reference map of the human binary protein interactome. *Nature* **580**, 402-408.

Nam, M. W., Kim, C. W. and Choi, K. C. (2022) Epithelial-mesenchymal transition-inducing factors involved in the progression of lung cancers. *Biomol. Ther. (Seoul)* **30**, 213-220.

Peart, O. (2017) Metastatic breast cancer. *Radiol. Technol.* **88**, 519M-539M.

Persaud, A., Alberts, P., Amsen, E. M., Xiong, X., Wasmuth, J., Saadon, Z., Fladd, C., Parkinson, J. and Rotin, D. (2009) Comparison of substrate specificity of the ubiquitin ligases Nedd4 and Nedd4-2 using proteome arrays. *Mol. Syst. Biol.* **5**, 333.

Rho, S. B., Byun, H. J., Kim, B. R. and Lee, C. H. (2021a) Knockdown of LKB1 sensitizes endometrial cancer cells via AMPK activation. *Biomol. Ther. (Seoul)* **29**, 650-657.

Rho, S. B., Lee, K. W., Lee, S. H., Byun, H. J., Kim, B. R. and Lee, C. H. (2021b) Novel anti-angiogenic and anti-tumour activities of the N-terminal domain of NOEY2 via binding to VEGFR-2 in ovarian cancer. *Biomol. Ther. (Seoul)* **29**, 506-518.

Rolland, T., Tasan, M., Charloteaux, B., Pevzner, S. J., Zhong, Q., Sahni, N., Yi, S., Lemmens, I., Fontanillo, C., Mosca, R., Kamburov, A., Ghiassian, S. D., Yang, X., Ghamsari, L., Balcha, D., Begg, B. E., Braun, P., Brehme, M., Broly, M. P., Carvunis, A. R., Convery-Zupan, D., Corominas, R., Coulombe-Huntington, J., Dann, E., Dreze, M., Dricot, A., Fan, C., Franzosa, E., Gebreab, F., Gutierrez, B. J., Hardy, M. F., Jin, M., Kang, S., Kiros, R., Lin, G. N., Luck, K., MacWilliams, A., Menche, J., Murray, R. R., Palagi, A., Poulin, M. M., Rambout, X., Rasla, J., Reichert, P., Romero, V., Ruyssinck, E., Sahalie, J. M., Scholz, A., Shah, A. A., Sharma, A., Shen, Y., Spirohn, K., Tam, S., Tejeda, A. O., Trigg, S. A., Twizere, J. C., Vega, K., Walsh, J., Cusick, M. E., Xia, Y., Barabási, A. L., Iakoucheva, L. M., Aloy, P., De Las Rivas, J., Tavernier, J., Calderwood, M. A., Hill, D. E., Hao, T., Roth, F. P. and Vidal, M. (2014) A proteome-scale map of the human interactome network. *Cell* **159**, 1212-1226.

Snezhkina, A., Lukyanova, E., Fedorova, M., Kalinin, D., Melnikova, N., Stepanov, O., Kiseleva, M., Kaprin, A., Pudova, E. and Kudryavtseva, A. (2019) Novel genes associated with the development of carotid Paragangliomas. *Mol. Biol.* **53**, 547-559.

Suh, Y., Yoon, C., Kim, R., Lim, E., Oh, Y., Hwang, S., An, S., Yoon, G., Gye, M., Yi, J., Kim, M. J. and Lee, S. J. (2013) Claudin-1 induces epithelial–mesenchymal transition through activation of the c-Abl-ERK signaling pathway in human liver cells. *Oncogene* **32**, 4873-4882.

Wang, J., Rouse, C., Jasper, J. S. and Pendergast, A. M. (2016) ABL kinases promote breast cancer osteolytic metastasis by modulating tumor-bone interactions through TAZ and STAT5 signaling. *Sci. Signal.* **9**, ra12.

Wang, W., Li, M., Ponnusamy, S., Chi, Y., Xue, J., Fahmy, B., Fan, M., Miranda-Carboni, G. A., Narayanan, R., Wu, J. and Wu, Z. H. (2020) ABL1-dependent OTULIN phosphorylation promotes genotoxic Wnt/β-catenin activation to enhance drug resistance in breast cancers. *Nat. Commun.* **11**, 3965.

Xu, X., Zhang, M., Xu, F. and Jiang, S. (2020) Wnt signaling in breast cancer: biological mechanisms, challenges and opportunities. *Mol. Cancer* **19**, 165.

Yamamoto, K., Gandin, V., Sasaki, M., McCracken, S., Li, W., Silvester, J. L., Elia, A. J., Wang, F., Wakutani, Y., Alexandrova, R., Oo, Y. D., Mullen, P. J., Inoue, S., Itsumi, M., Lapin, V., Haight, J., Wakeham, A., Shahinian, A., Ikura, M., Topisirovic, I., Sonenberg, N. and Mak, T. W. (2014) Largen: a molecular regulator of mammalian cell size control. *Mol. Cell* **53**, 904-915.

Zandy, N. L. and Pendergast, A. M. (2008) Abl tyrosine kinases modulate cadherin-dependent adhesion upstream and downstream of Rho family GTPases. *Cell Cycle* **7**, 444-448.

Zandy, N. L., Playford, M. and Pendergast, A. M. (2007) Abl tyrosine kinases regulate cell-cell adhesion through Rho GTPases. *Proc. Natl. Acad. Sci. U.S.A.* **104**, 17686-17691.